10th International IFAC Symposium on
Computer Applications in Biotechnology
Preprints Vol.2, June 4-6, 2007, Cancún, Mexico

MODELLING AND IDENTIFICATION OF AERATION SYSTEMS FOR MODEL PREDICTIVE CONTROL OF DISSOLVED OXYGEN – SWARZEWO WASTEWATER TREATMENT PLANT CASE STUDY

W. Krawczyk [*] **R. Piotrowski** [*] **M.A. Brdys** [*] [**] **W. Chotkowski** [*]

[*] *Department of Automatic Control, Gdansk University of Technology, ul. G. Narutowicza 11/12, 80 952 Gdansk, Poland, email: wal_niety@wp.pl, r.piotrowski@ely.pg.gda.pl, w.chotkowski@chello.pl*

[**] *Department of Electronic, Electrical and Computer Engineering, The University of Birmingham, Birmingham B15 2TT, UK, email:m.brdys@bham.ac.uk*

Abstract: Aeration is an important and expensive activity that is carried out during wastewater treatment plant (*WWTP*) operation. The aeration system serves as the actuator to deliver the airflow prescribed by the dissolved oxygen controller. It is on its own a complex dynamic system with nonlinear hybrid dynamics. Recently hybrid model predictive controllers (*HMPC*) were proposed in order to control the system valve and blower operation so that the required airflow can be accurately delivered and the energy cost due to blowing the air minimised. Availability of a suitable model of the aeration system is vital for a successful operation of these controllers. The paper improves the model recently proposed. A practical approach to the model identification and validation is proposed and applied to Swarzewo *WWTP*. *Copyright © 2007 IFAC*

Keywords: air, biotechnology, dynamic systems, identification, modelling, nonlinear systems, verification, waste treatment.

1. INTRODUCTION

Maintaining *DO* concentration aerobic zones at a right level corresponding to variations of the *WWTP* influent flow and pollutant concentrations is vital for the plant desired operation (Olsson and Newell, 1999). A control structure and algorithms were proposed in (Grochowski, *et. al.,* 2004) to generate on line the *DO* optimised trajectory. Design of a controller that uses airflow into the aerobic zone as a manipulated variable to achieve the prescribed *DO* level been the subject of the numerous papers (Lindberg and Carlsson, 1996; Olsson and Newell, 1999; Yoo, *et. al.,* 2002; Brdys and Diaz-Maiquez, 2002; Sanchez and Katebi, 2003; Piotrowski, *et. al.,* 2004; Chotkowski, *et. al.,* 2005; Piotrowski and Brdys, 2005). The airflow calculated by the *DO* controller is to be provided by the aeration system. Hence, the aeration system serves as the *DO* controller actuator. It is on its own a complex dynamic system with hybrid nonlinear dynamics. Its operation is expensive due to cost of electrical energy used to blow the air into the aerobic zones. Recently a *HMPC* was proposed in order to control the system valve and blower operation so that the required airflow can be accurately delivered and the energy cost due to blowing the air is minimised (Brdys, *et. al.,* 2002; Piotrowski and Brdys, 2005). Availability of a suitable model of the aeration system is vital for a successful operation of the *HMPC*. The paper improves the model recently proposed. A practical approach to the model identification and validation is proposed and applied to Swarzewo *WWTP* case study. The paper is organised as follows. The Swarzewo *WWTP* case study is described in section 2 and the aeration system is presented in details. The improved model suitable for the *HMPC* application is

derived in section 3. The model identification and validation tests for the case study system are presented in section 4. Section 5 concludes the paper.

2. PRESENTATION OF THE CASE STUDY WASTEWATER TREATMENT PLANT AND AERATION SYSTEM

2.1 Wastewater treatment plant at Swarzewo

The wastewater treatment plant in Swarzewo, Northern Poland, employs an activated sludge biological wastewater treatment that is supported by standard mechanical activities. The biological pollutant removal is performed by four Sequential Batch Reactors (*SBR*). The *SBR* volumes are: *SBR* 1, 2, 3 are of 5100 m^3, *SBR* 4 is of 6400 m^3. The effluent is released to Baltic Sea. The plant technological layout is shown in Fig. 1.

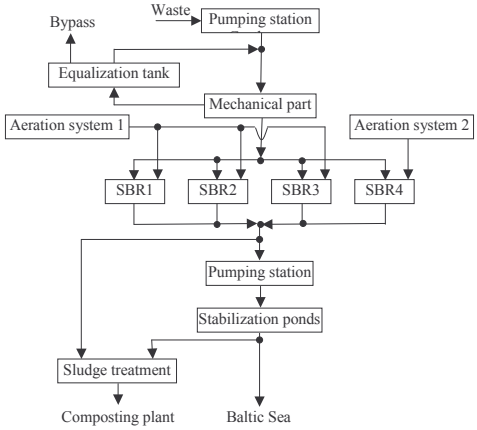

Fig.1. Technological layout of Swarzewo WWTP.

The *SBR* operate in parallel and independently. A single *SBR* cycle consists of the following sequentially performed operations: loading, aeration, sedimentation and decantation.

2.2 The aeration system

The aeration system delivers airflow and therefore oxygen needed for biological pollutant removal from the wastewater. It is composed of the blower station, diffuser system and interconnected pipes. There are two independent aeration systems at the *WWTP* (see Fig.1) and the paper considers modelling the system 2 for model predictive control purposes. With the existing sensor accessibility modelling the system 1 was not possible. The modelled aeration system is composed of two identical variable speed blowers that are powered by inverters. Single blower airflow can be reliably controlled within range of 1440 – 3157 m^3/h. The pumped airflow moves into a common collector. The airflow splits from the collector into two airflows into two pipes that deliver the air to the diffuser systems located at the bottom floor of biological reactor. This is illustrated in Fig. 2 where the two parallel aeration segment units are shown.

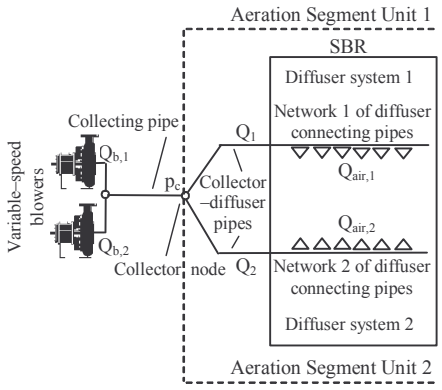

Fig. 2. The case – study aeration system.

Each of them is composed of the collector - diffuser pipe and diffuser system. The diffuser system is composed of a number of diffusers in parallel located at the reactor bottom floor and connected through a network of secondary pipes to the collector - diffuser pipe (see Fig. 2). The pipe diameters decrease over a distance about 65m from the blower station to the diffuser systems from 600 to 200 mm.
The diffusers are membrane disk type. There are 616 and 600 diffusers in the diffuser systems 1 and 2, respectively. They operate in parallel and their distribution is shown in Fig. 3. In order to maintain a diffuser open the pressure drop across the diffuser should not be smaller than 2 kPa.

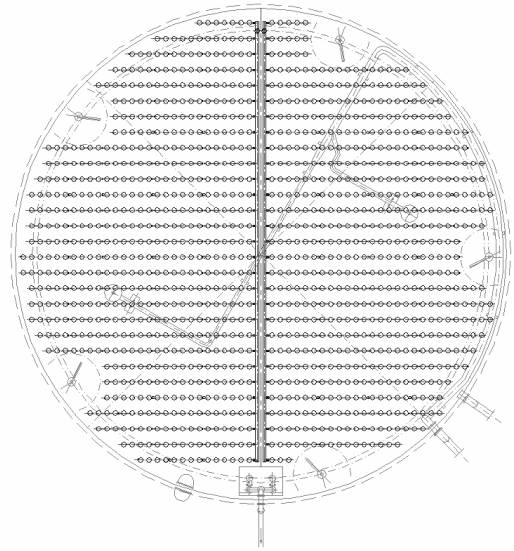

Fig. 3. Distribution of diffusers.

3. MODELLING THE AERATION SYSTEM

The model derived in (Brdys, *et. al.,* 2002) will be further improved and applied to the case study aeration system.

3.1 Blowers

We shall start with the blower modelling. For each of the two variable speed blowers the relationship between pressure drop across a blower $\Delta p_{b,i}$ and the airflow through the blower $Q_{b,i}$ can be written as:

$$Q_{b,i} = f_{b,i}\left(x_{b,i}, \Delta p_{b,i}, n_{b,i}\right);\ i \in \{1, 2\},\ x_{b,i} \in \{0,1\} \quad (1)$$

where $n_{b,i}$ is a motor rotational speed; $x_{b,i} = 1$ if the blower in *on* and $x_{b,i} = 0$ if the blower is *off*.

The blower station model is obtained in a straightforward manner by utilising the blower models (1) and the parallel station structure:

$$Q_b = f_b\left(\boldsymbol{x_b}, \boldsymbol{\Delta p_b}, \boldsymbol{n_b}\right) = \sum_{i \in \{1, 2\}} f_{b,i}\left(x_{b,i}, \Delta p_{b,i}, n_{b,i}\right) \quad (2)$$

where Q_b, Δp_b, n_b are the overall airflow into the blower node, pressure drop across at the blower station and motor rotational speeds, respectively.

Moreover, the following hold:

$$\Delta p_b = p_b - p_a = \Delta p_{b,i};\ i \in \{1, 2\} \quad (3)$$

$$\boldsymbol{x_b} = \left[x_{b,1}, x_{b,2}\right], \boldsymbol{n_b} = \left[n_{b,1}, n_{b,2}\right],\ i \in \{1, 2\} \quad (4)$$

where p_b, p_a are the pressure at the blower station node and atmospheric pressure, respectively; the binary vector $\boldsymbol{x_b}$ defines which of the blowers are *on* and *off*. Hence, the vector variable $\boldsymbol{x_b}$ defines the blower station operating structure.

The functions $f_{b,i}(\cdot)$ are nonlinear and available from manufacturer data.

Connecting the blowers to collector pipe introduces certain fluid resistance R_r that is modelled as:

$$\Delta p_r = f_r\left(Q_b\right) = R_r(Q_b) Q_b \ \ and \ \ R_r\left(Q_b\right) = \frac{\Delta p_r}{Q_b} \quad (5)$$

where Δp_r is the pressure drop across the blower-collector pipe connection.

The collector pressure p_c can now be expressed as:

$$p_c = \Delta p_{b,i} - \Delta p_r + p_a = p_b - \Delta p_r \quad (6)$$

3.2 Collector pipe

The collector pipe (see Fig. 2) pipe is treated as the fluid flow capacitance. Applying a standard mass balance principle at the collector node yields:

$$\frac{dp_c}{dt} = \frac{1}{C_c}\left(Q_b - Q_c\right) \text{ and } C_c = k_c \cdot V_c \cdot p_c;\ V_c = \frac{\Pi \cdot d_c^2}{4} \cdot l_c \quad (7)$$

where C_c, Q_c, V_c, p_c, d_c, l_c are the collector fluid flow capacitance, collector flow, collector volume, collector diameter and collector length, respectively; the unit conversion coefficient $k_c = 1\dfrac{m^2 s^4}{kg^2}$.

In this case study $l_c = 44{,}11\,m$ and $d_c = 0{,}6\,m$. Notice that the fluid resistance in the collector pipe is neglected in (7) as it was founded out small.

3.3 Aeration segment units

The airflow leaving the collector node is delivered to the aerobic zones by two aeration segment units (see Fig. 2). For modelling purposes all diffusers in each diffuser system are aggregated into a single equivalent diffuser. Hence, each aeration segment unit is modelled as a fluid flow capacitance $C_{d,j}$ catering for the collector - diffuser pipe and secondary pipe network capacities with two resistances $R_{g,j}$, $R_{d,j}$. The resistance $R_{g,j}$ concerns the collector - diffuser pipe together with the pipe network while the resistance $R_{d,j}$ concerns the diffuser. This is followed by a hydrostatic pressure of wastewater in the reactor. The system and its electrical analogy is illustrated in Fig. 4.

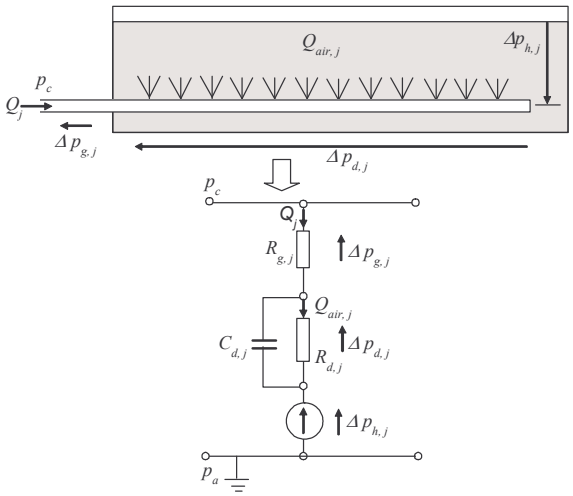

Fig. 4. The aeration segment unit and its electrical analogy.

Based on the manufacturer data it was found that

$$\Delta p_{g,j} = e_j \cdot Q_j^2 \text{ and } R_{g,j} = \frac{\Delta p_{g,j}}{Q_j};\ \ j \in \{1,2\} \quad (8)$$

where $e_1 = 8{,}664816 \cdot 10^{-9}$, $e_2 = 1{,}6216792 \cdot 10^{-8}$.

Let us now consider the equivalent diffuser resistance $R_{d,j}$ (see Fig 4). We shall start with the diffuser system that is composed of one diffuser only. In the steady-state the open diffuser airflow – pressure drop link is described by a nonlinear function $Q_{air,j} = f_{d,j}(\Delta p_{d,j})$. If the pressure drop falls bellow certain value $\Delta p_{d,j}^{open}$ then the diffuser closes and $Q_{air,j} = 0$. Hence, the following holds:

$$Q_{air,j} = \begin{cases} f_{d,j}\left(\Delta p_{d,j}\right) & for\ \Delta p_{d,j} \geq \Delta p_{d,j}^{open} \\ 0 & otherwise \end{cases};\ \ j \in \{1, 2\} \quad (9)$$

The nonlinear function $f_{d,j}$ obtained from the manufacturer data was linearised by a standard linear regression to produce:

$$Q_{air,j} = \begin{cases} \dfrac{\Delta p_{d,j} - \Delta p_{d,j}^{open}}{R_{d,j}} & for\ \ \Delta p_{d,j} \geq \Delta p_{d,j}^{open} \\ 0 & otherwise \end{cases};\ \ j \in \{1,2\} \qquad (10)$$

where $R_{d,j} = 0,74\left[\dfrac{kPa \cdot h}{m^3}\right]$; $\Delta p_{d,j}^{open} = 2\,kPa$; $j \in \{1,2\}$.

As there are n_j, $j \in \{1,2\}$ diffusers in parallel within each of the diffuser systems the relationship (10) describing a single diffuser can be utilised according to: $Q_{air,j} := n_j\, Q_{air,j}$ and $\Delta p_{d,j} := \Delta p_{d,j}$ to produce the linearised relation (9) for the equivalent diffuser:

$$Q_{air,j} = \begin{cases} n_j \dfrac{\Delta p_{d,j} - \Delta p_{d,j}^{open}}{R_{d,j}} & for\ \ \Delta p_{d,j} \geq \Delta p_{d,j}^{open} \\ 0 & otherwise \end{cases};\ \ j \in \{1,2\} \qquad (11)$$

Hence, the equivalent diffuser pressure drop – airflow relation is obtained by reducing the single diffuser resistance by dividing it by a number of diffusers with the diffuser system. The opening pressure drop remains the same.
Finally, the diffuser airflow dynamics can be described as (see Fig. 4):

$$R_{d,j}\, C_{d,j} \frac{dQ_{air,j}}{dt} + Q_{air,j} = Q_j;\ \ j \in \{1,2\} \qquad (12)$$

As the diffuser outflow pressure $p_{d,j}$ is nearly constant the $C_{d,j}$ can also be treated as a constant value and

$$C_{d,j} = k_{d,j} \cdot V_{d,j} \cdot p_{d,j};\ \ j \in \{1,2\} \qquad (13)$$

where $V_{d,j}$ is a volume of the collector – diffuser pipe together with the pipe network and the unit conversion coefficients $k_{d,j} = k_c$.

The volume is expressed as an equivalent pipe volume with the diameter $d_{d,j}$ and length $l_{d,j}$. Hence,

$$V_{d,j} = \frac{\Pi \cdot d_{d,j}^2}{4} \cdot l_{d,j};\ \ j \in \{1,2\} \qquad (14)$$

The equivalent pipe diameter was calculated as the weighted sum of the diameters of the collector – diffuser pipe and the network pipe diameters to produce: $d_{d,1} = 0,10237\,m$ and $d_{d,2} = 0,10256\,m$. The equivalent pipe length was calculated as a sum of the collector – diffuser pipe length and a total length of the network pipes to produce: $l_{d,1} = 426,5115\,m$ and $l_{d,2} = 417,2315\,m$. The hydrostatic pressure in an aeration tank is modelled as:

$$\Delta p_{h,j} = \rho \cdot g \cdot h_j;\ \ j \in \{1,2\} \qquad (15)$$

where ρ, g, h_j are the wastewater density at aeration tank, gravity acceleration and height of diffuser in wastewater at aeration tank, respectively.
As h_j is typically constant $\Delta p_{h,j}$ is constant as well and $h_j = 6,25\,m$ in our case study system.

A pressure drop across the aeration segment unit with a diffuser that is open is described by the equation coupling pressures in the overall system (see Fig. 4):

$$p_c - p_a = \Delta p_{g,j} + \Delta p_{d,j} + \Delta p_{h,j};\ \ j \in \{1,2\} \qquad (16)$$

The input and output airflow temperatures in the aeration system can signicantly differ. Hence, the temperature differences in the input and output of the main collector pipe T_1, T_2 and in the input and output of the aeration segment pipes T_3, T_4 are taken into account in the model assuming constant air volume in the corresponding pipes as:

$$p_c = p_b \cdot \frac{T_2}{T_1} \qquad (17)$$

and

$$Q_1 = \frac{T_3}{T_2} \cdot \left(p_c - p_{d,1}\right) \cdot \frac{1}{R_{g,1}};\ Q_2 = \frac{T_4}{T_2} \cdot \left(p_c - p_{d,2}\right) \cdot \frac{1}{R_{g,2}} \qquad (18)$$

These expressions are applied to correct the pressures and airflows currently obtained from the model without temperature involved. Here, the temperature values in the above correction formulae are taken from the measurements and this limits applicability of these corrections to model predictive control. The temperature dynamics model is also required but this is beyond the paper scope.

3.4 Overall model

A circuit in Fig. 5 is an electrical analogy of the aeration system model. Collecting the formulae describing the system elements as above and connecting them as shown in the circuit produces the overall model equations.

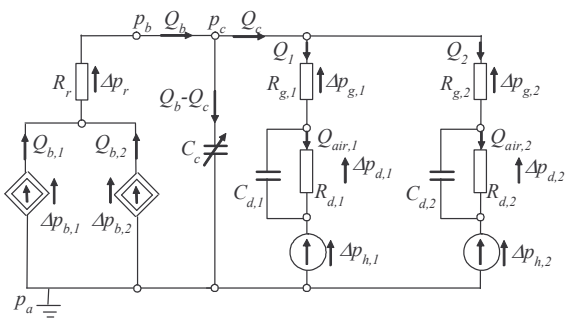

Fig. 5. Electrical analogy of the aeration system model.

4. MODEL IDENTIFICATION AND VALIDATION

The structure and parameterization of the model derived in section 3 were based on well known physical principles and the case study system structure. Certain model element characteristics were taken from a manufacturer data sources. Other parameters such as the resistances and capacitances were calculated based on the element geometrical dimensions by applying well known formulae. However, the model elements typically describe the physical elements that are spatially distributed in the real system. Hence, the appropriateness of the lumped parameter model needs to be validated. First the model identification will be carried out element by element. Next an overall model will be validated by comparing the model responses with the sensor measurements across an overall system. The airflows $Q_{air,1}$, $Q_{air,2}$ being the system outputs are the manipulated variables for a *DO* controller (Chotkowski, *et. al.,* 2005). Their direct sensor measurements are not available when the system operates in a truly dynamic mode. Hence, the model will be identified by comparing the intermediate flow and pressure measurements with the corresponding model responses.

4.1 Selection of sensors and location of the measurement points

The pressure, fluid flow and temperature sensors were chosen. Their location is illustrated in Fig. 6. It reflects a trade off between the costs and quality of the measurement information and also meets requirements for the measurement correctness. The measurements p_1, T_1 and p_2, T_2 are carried out as close to the ends of the collector pipe as possible. In a similar manner the measurements p_3, T_3 and p_4, T_4 are performed with regard to the collector-diffuser pipes. The collector pipe airflow Q_c sensor was placed in the mid of the collector pipe in order to make sure that the sensor in located at a straight line segment of the collector pipe sufficiently far from its ends. The routine sensors at the blower station delivered measurements of the blower airflows, frequencies of the invertors used to calculate the blower speeds, pressure drops across the blowers and temperature of the input air flow into the blowers.

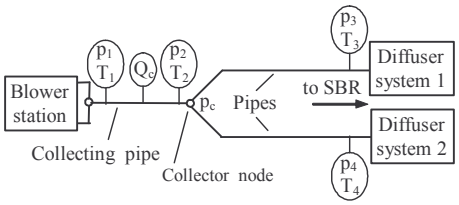

Fig. 6. Location of the measurement points.

4.2 Identification results

The blower – collector pipe connecting resistance

The resistance R_r was experimentally determined from the measurements of Δp_r and Q_b the results are illustrated in Fig. 7 to show a linear resistance – airflow dependence.

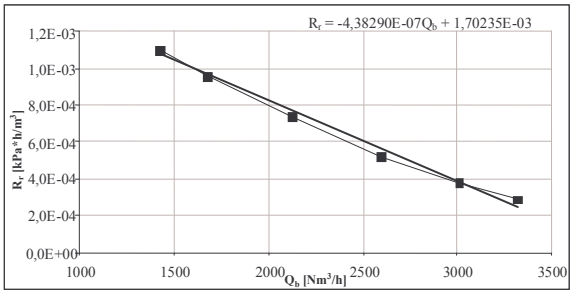

Fig. 7. The blower – collector pipe connecting resistance – airflow relationship.

Collector pipe dynamics

A trapezoidal change of one blower airflow $Q_{b,i}$ from 50% to 100% made over about 12 sec period with the remaining blower being turned off was the best that could be achieved in producing a step input signal into the collector pipe system with the dynamics modelled by (9). The resulting collector pipe airflow measurements are illustrated in Fig. 8. The rate of change of the measured airflow in the collector pipe is of the same order as produced by the model. As dynamics of the biological processes is much slower then such model accuracy is sufficient for the *DO* control purposes.

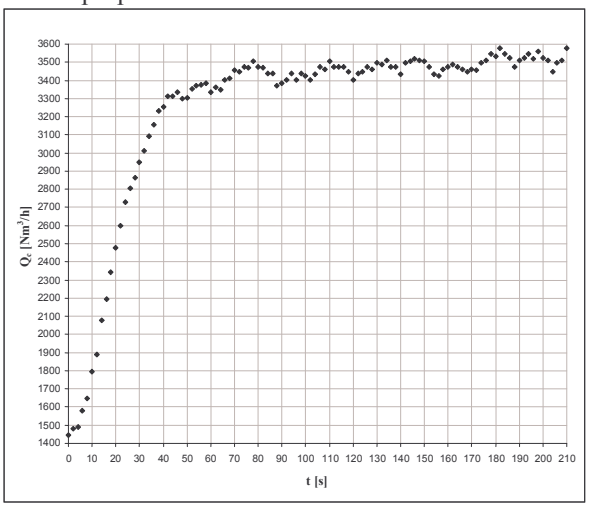

Fig. 8. Response of collector pipe to blower trapezoidal airflow input.

An overall system model verification results under steady – state operation

Finally, the interconnected aeration system was exercised by piecewise constant motor speed input and the corresponding steady-state responses were recorded. The results are shown in Table 1.

Table 1 Identification results for an overall model: measurements and model-measurement errors

n [rev/min]	p_b [kPa]	p_1 [kPa]	p_2 [kPa]	p_3 [kPa]	p_4 [kPa]	Q_c [m^3/h]
30000	73,03	71,42	71,18	71,17	71,17	1628
30312	73,56	71,94	71,52	71,51	71,5	2176
30630	73,66	72,16	71,74	71,72	71,72	2533
30948	73,65	72,3	71,89	71,87	71,86	2778
31560	73,57	72,68	72,19	72,17	72,15	3256
32040	73,53	72,7	72,23	72,2	72,19	3313

n [rev/min]	error p_b [%]	error p_1 [%]	error p_2 [%]	error p_3 [%]	error p_4 [%]	error Q_c [%]
30000	-0,91	-1,16	-2,06	-1,78	-2,08	14,68
30312	-0,46	-0,66	-1,97	-1,53	-1,87	20,08
30630	-0,73	-0,82	-1,97	-1,67	-1,94	19,14
30948	-0,74	-0,90	-2,06	-1,68	-1,99	6,94
31560	-0,98	-0,76	-1,89	-1,57	-1,81	8,18
32040	-1,04	-0,98	-2,10	-1,77	-1,94	-0,30

4.3 Validation results

This model was validated based on the steady – state responses. The validation results are shown in Table 2.

Table 2 Validations of an overall model: measurements and model - measurement errors

n [rev/min]	p_b [kPa]	p_1 [kPa]	p_2 [kPa]	p_3 [kPa]	p_4 [kPa]	Q_c [m^3/h]
28128	63,08	61,49	61,33	61,32	61,32	1569
28332	63,29	61,64	61,48	61,47	61,47	1810
28752	63,6	62,02	61,83	61,81	61,8	2364
29226	63,66	62,33	62,09	62,07	62,06	2791
30000	63,61	62,69	62,37	62,34	62,33	3234
30780	63,51	62,83	62,49	62,46	62,45	3431

n [rev/min]	error p_b [%]	error p_1 [%]	error p_2 [%]	error p_3 [%]	error p_4 [%]	error Q_c [%]
28128	0,61	-0,28	-0,08	-0,52	-0,68	-0,59
28332	0,62	-0,39	-0,19	-0,57	-0,79	-4,19
28752	0,95	-0,06	0,08	-0,31	-0,48	0,13
29226	1,05	0,05	0,18	-0,27	-0,42	-5,42
30000	0,97	0,30	0,18	0,00	-0,21	4,69
30780	0,49	0,34	0,18	-0,03	-0,18	-3,59

Comparing the results in the Table 1 with the results in Table 2 we shall notice that the model validation results are better than the verification ones. The maximal pressure residuum is around 1% while the maximal airflow residuum is about 5%.

5. CONCLUSIONS

Modelling the aeration system for control purpose has been pursued in the paper. The recently derived model has been further improved by applying modified formula for calculating the pipe capacitances. It has been demonstrated that incorporating temperature changes along the system improves the model accuracy. Deriving the temperature model is under the research. The model structure, its parameterisation and approach to the parameter calculation from the manufacturer data have been successfully validated by application to the case study system. The tedious parameter value calculations for complex systems need to be replaced by recursive parameter estimation technique and this is also under current research.

REFERENCES

Brdys, M.A., W. Chotkowski, K. Duzinkiewicz, K. Konarczak and R. Piotrowski (2002). Two-level dissolved oxygen control for activated sludge processes. *Proc. of the 15th IFAC World Congress,* Barcelona, July 21-26.

Brdys M.A. and J. Diaz-Maiquez (2002). Application of fuzzy model predictive control to the dissolved oxygen concentration tracking in an activated sludge process. *Proc. of the 15th IFAC World Congress*, Barcelona, July 21-26.

Chotkowski W., M.A. Brdys and K. Konarczak (2005). Dissolved oxygen control for activated sludge processes. *International Journal of System Science,* **Vol. 36, No. 12,** pp. 727-736.

Grochowski, M., M.A. Brdys and T. Gminski (2004). Intelligent control structure for control of integrated wastewater systems. *Proc. of the 10th IFAC Symposium Large Scale Systems: Theory and Applications.* Osaka, July 26-28.

Lindberg, C.F. and B. Carlsson (1996). Nonlinear and set-point control of the dissolved oxygen concentration in an activated sludge process. *Wat. Sci. Tech*., **34**(**3-4**), pp. 135-142.

Olsson, G. and R. Newell (1999). *Wastewater Treatment Systems. Modelling, Diagnosis and Control.* IWA Publishing, London.

Piotrowski, R., K. Duzinkiewicz and M.A. Brdys (2004). Dissolved oxygen tracking and control of blowers at fast time scale. *Proc. of the 10th IFAC Symposium Large Scale Systems: Theory and Applications*. Osaka, July 26-28.

Piotrowski, R. and M.A. Brdys (2005). Lower-level controller for hierarchical control of dissolved oxygen concentration in activated sludge processes. *Proc. of the 16th IFAC World Congress*. Prague, July 04-08.

Sanchez A. and M.R. Katebi (2003). Predictive control of dissolved oxygen in an activated sludge wastewater treatment plant. *Proc. of the European Control Conference ECC'2003*, Cambridge, UK.

Yoo C.K., H.K. Lee and I. Beum Lee (2002). Comparison of process identification methods and supervisory control in the full scale wastewater treatment plant. *Proc. of the 15th IFAC World Congress*, Barcelona, July 21-26.